

# An Inverse Problem Approach to Extract the Growth Kernel in Particulate Processes<sup>★</sup>

Ala Eldin Bouaswaig\* Sebastian Engell\*\*

\* *Process Dynamics and Operations Group, Technische Universität  
Dortmund, 44221 Dortmund, Germany (e-mail:  
ala.bouaswaig@udo.edu).*

\*\* *Process Dynamics and Operations Group, Technische Universität  
Dortmund, 44221 Dortmund, Germany (e-mail:  
s.engell@bci.tu-dortmund.de)*

---

**Abstract:** Mathematical models of particulate processes usually include a population balance equation to describe the dynamics of the size distribution. The structure of the population balance equation is the same in all models of particulate processes and the specific physical and chemical interaction of the particles is described by individual kernels. Usually first principles modeling is used to develop the kernels, but in cases in which this is intractable, inverse problem techniques have been proposed in the literature to extract the kernels from experimental data. In this work we introduce an approach that can be used for extracting the growth kernel. This approach is applicable even when the assumption of separable growth rate that has been made in previous approaches does not hold and when coagulation with known dynamics and growth are taking place simultaneously.

*Keywords:* Population balance equation; Particulate processing; Inverse dynamic problem; Growth; Neural-network models

---

## 1. INTRODUCTION

Due to the dependency of the end-use properties of particulate products such as crystals and polymers on their size distribution, modeling and control of the size distribution is of extreme interest. Such modeling tasks are complicated because of the interaction of several physical and chemical phenomena that take place simultaneously in these processes. These phenomena include nucleation, growth, coagulation and breakage. In the literature, models ranging from fundamental to black box models for particulate processes exist. First principles models mainly use the population balance equation (PBE) to describe the dynamics of the size distribution. The complete model of the process comprises the PBE with the other balance equations for the continuous phase variables in the system (Alhamad et al., 2005; Immanuel et al., 2002; Rajabi-Hamane and Engell, 2007). In many cases however, models for the individual kernels in the PBE are either unavailable or unreliable and researchers use input output data to construct data based models (Dokucu and Doyle III, 2008; Dokucu et al., 2008). Due to the inflexibility of such black box models and the complexity and the above mentioned limitations of rigorous models in particulate processes other intermediate approaches between the two extremes have been proposed. These approaches maintain the main

structure of the fundamental model (i.e. the PBE) and aim at developing models for the individual kernels by applying inverse problem techniques; i.e., the individual kernels are extracted from measured data. Such intermediate models partly sacrifice rigorousness but simultaneously maintain, to some extent, flexibility and occasionally even improve versatility.

Inverse problem approaches to the modeling of particulate processes have been applied for extracting the nucleation and growth kernel (Mahoney et al., 2000, 2002; Ramkrishna, 2000), the coagulation kernel (Ramkrishna, 2000; Wright and Ramkrishna, 1992) and the breakage kernel (Ramkrishna, 2000). This work is a further contribution in this direction and it presents a novel method that extends the approach proposed by Mahoney et al. (2000, 2002) for extracting the growth kernel. The approach is applied first to two test problems. Thereafter, the application of the method for extracting the growth kernel in emulsion polymerization, both with and without co-occurring coagulation with known dynamics, is presented.

The remainder of the paper is structured as follows: In Section 2, the original approach proposed by Mahoney et al. (2002) for extracting the growth kernel is briefly explained, the proposed method is presented and the extension over the existing method is highlighted. The results obtained when the method is applied to test problems and to the emulsion polymerization problem are demonstrated

---

<sup>★</sup> The financial support of the General People's Committee for Higher Education (Libya) and of The Graduate School of Production Engineering and Logistics (Technische Universität Dortmund) is gratefully acknowledged.

in Sections 3 and 4. Finally, Section 5 is devoted to drawing conclusions and indicating prospects for future research.

## 2. THEORY

The PBE that describes simultaneous growth and coagulation is given by

$$\frac{\partial n_v(v, t)}{\partial t} + \frac{\partial(G_v(v, t)n_v(v, t))}{\partial v} = \mathfrak{R}_{coag}(v, t), \quad (1)$$

where  $n_v(v, t)$  is the number density function and  $n_v(v, t)dV$  represents the number of particles per unit volume with sizes between  $V$  and  $V + dV$ .  $G_v(v, t)$  and  $\mathfrak{R}_{coag}(v, t)$  are the growth and coagulation kernels. Our objective here is to extract the growth kernel from measured data. As mentioned previously, this issue has first been addressed by Mahoney et al. (2000, 2002). We begin by briefly explaining the original approach and highlighting the main assumption made in it. The modification that is proposed to make it possible to handle more general cases in which these assumptions are not valid is presented in Section 2.2.

### 2.1 Separable growth rate

Mahoney et al. (2000, 2002) considered the case where no coagulation takes place. If constant ordering holds (i.e. the growth rate is deterministic and well mixed conditions can be assumed) the characteristics of the PBE can be extracted from the experimental data.

The main assumption in this approach is that the growth rate is separable; that is:

$$G_v(v, t) = G_1(v)G_2(t). \quad (2)$$

Since the quantity  $G_1(v)n_v(v, t)$  is conserved along the characteristics (Mahoney et al., 2002), the procedure for extracting the growth kernel is as follows:

**Step 1.** Approximate the functions  $G_1(v)$  and  $G_2(t)$  by polynomials.

**Step 2.** Making use of the conservation of the quantity  $G_1(v)n_v(v, t)$ , determine the unknown coefficients of the polynomial  $G_1(v)$  by performing a linear least squares optimization of the following set of equations:

$$\begin{aligned} n_{v,1,k}G_1(v_{1,k}) &= n_{v,2,k}G_1(v_{2,k}) \\ &= \dots = n_{v,\tau,k}G_1(v_{\tau,k}), \end{aligned}$$

where  $k \in [1, M]$ ,  $M$  is the total number of tracked characteristics and  $\tau$  is the number of time instances at which the measurements are available.

**Step 3.** Determine the coefficients of the polynomial  $G_2(t)$  by solving the following set of equations:

$$\int_{v_0}^{v(t|v_0, t_0)} \frac{dv}{G_1(v)} = \int_{t_0}^t G_2(t)dt, \quad (3)$$

where  $v(t|v_0, t_0)$  represents the location of the characteristic at time  $t$  that initially was located at  $v_0$ .

Mahoney et al. (2002) used local cubic basis functions to approximate both  $G_1(v)$  and  $G_2(t)$ . The approach was tested on a test problem, a simulated precipitation system, and an emulsion polymerization example (Mahoney et al.,

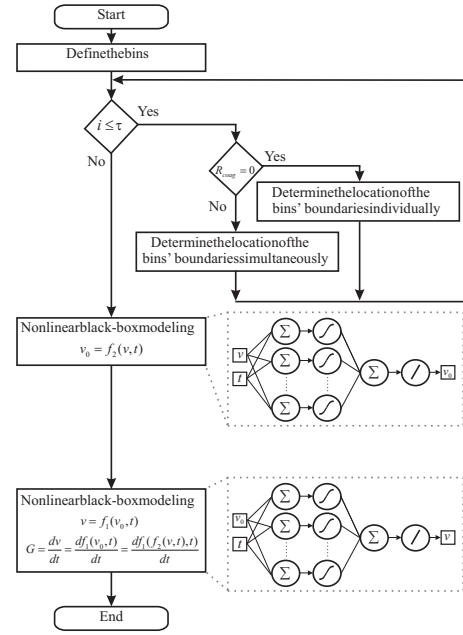


Fig. 1. Flowchart of the proposed algorithm.  $i$  is the index of the time instances at which the measurements are available.

2000, 2002). The results in the former two cases were good. In the latter case, however, the time span of the experiment had to be split into two intervals and a separate growth kernel had to be generated for each interval to obtain good results.

### 2.2 General growth rate

The algorithm proposed in this paper is illustrated in Fig. 1 and is more general since it can be applied without having to impose any preconditions on the structure of the growth kernel. The core concept of both techniques, however, is the same; i.e. the characteristics are extracted from experimental data and a growth kernel is computed from this information.

The approach suggested here is based on the fixed pivot on a moving grid method (FPMG) of Kumar and Ramkrishna (1997). The main idea in FPMG is to define a number of bins and discretize the original PBE (Eq. 1) in terms of these. The evolution of the boundaries of the bins is determined by the growth kernel. Hence, the discretized PBE is given by:

$$\frac{dN_i(t)}{dt} = \mathfrak{R}_{coag}(v_i, t), \quad (4)$$

$$\frac{dv_i}{dt} = G_v(v_i, t), \quad (5)$$

where Eq. 5 describes the evolution of the characteristics of the PBE and  $N_i(t)$  represents the total number of particles in the bin  $i$  at time  $t$ :

$$N_i(t) = \int_{v_i}^{v_{i+1}} n_v(v, t)dv. \quad (6)$$

The coagulation term in Eq. 4 is given by:

$$\begin{aligned} \mathfrak{R}_{coag}(v_i, t) = & - \int_{v_i}^{v_{i+1}} n(v, t) dv \int_0^\infty n(\acute{v}, t) \beta(v, \acute{v}) d\acute{v} \\ & + \frac{1}{2} \int_{v_i}^{v_{i+1}} dv \int_0^v n(v - \acute{v}, t) n(\acute{v}, t) \beta(v - \acute{v}, \acute{v}) d\acute{v}. \end{aligned} \quad (7)$$

For a pure growth problem, the total number of particles contained in the moving bin remains constant since  $\mathfrak{R}_{coag}(v_i, t)$  is equal to zero. In contrast, for particles undergoing simultaneous growth and coagulation the total number of particles within each bin varies based on the coagulation rate. Making use of these facts, the proposed approach for extracting the growth kernel for a pure growth problem proceeds as follows:

**Step 1.** Discretize the known distribution at  $t = t_0$  into  $M$  bins.

**Step 2.** Calculate  $N_i$  for each bin using Eq. 6.

**Step 3.** At every instant of time  $t_k$ , at which the measurement of the number density function  $n_v(v, t)$  is available, move the boundaries of the bins such that Eq. 4 holds for each bin.

**Step 4.** Train a neural network or use any other nonlinear black-box modeling technique to approximate the function  $f_1$  which is defined as follows:

$$v = f_1(v_0, t), \quad (8)$$

$$G_v(v_0, t) = \frac{dv}{dt} = \frac{df_1(v_0, t)}{dt}. \quad (9)$$

The function  $f_1$  in Eq. 8 maps the initial location of the bin boundaries obtained in Step 1 and the time instances at which the measurements are available  $t_k$  to the location of the boundaries obtained in Step 3. That is, starting from an initial grid  $\mathbf{v}_0$ , Eq. 8 describes the evolution of the characteristics of the PBE. Eq. 9 consequently gives the extracted growth kernel. Since it is desired to have  $G_v(v, t)$  instead of  $G_v(v_0, t)$  an additional step is added to the above procedure:

**Step 5.** Train a neural network or use any other nonlinear black-box modeling technique to approximate the function  $f_2$  which is defined as follows:

$$v_0 = f_2(v, t). \quad (10)$$

By substituting  $v_0$  from Eq. 10 in Eq. 9 the growth kernel is obtained.

For the case of simultaneous growth and coagulation, assuming that the coagulation frequency  $\beta(v, \acute{v})$  is known, since  $\mathfrak{R}_{coag}(v_i, t) = f(N_1(t), N_2(t), \dots, N_M(t))$ , as can be deduced from Eq. 7, Step 3 of the procedure described above can be replaced by the following two steps:

**Step 3.1.** Discretize the time derivative on the LHS of Eq. 4 using the Crank-Nicolson method:

$$\begin{aligned} \frac{N_i^{k+1} - N_i^k}{\Delta t(k)} = \\ \frac{1}{2} (\mathfrak{R}_{coag}(v_i, t_{k+1}) + \mathfrak{R}_{coag}(v_i, t_k)) \quad i = 1, 2, \dots, M. \end{aligned}$$

**Step 3.2.** Solve the resulting set of  $M$  coupled nonlinear equations simultaneously.

For calculating  $\mathfrak{R}_{coag}(v_i, t)$  the expressions described by Kumar and Ramkrishna (1997) that guarantee preservation of number and mass are applied.

It is clear from the above description that, because of using neural networks for reconstructing the characteristics, any general shape of the growth kernel can theoretically be approximated with reasonable accuracy. Furthermore, since the characteristics are obtained based on the FPMG, handling the coagulation term becomes straightforward. This is demonstrated in the following sections.

### 3. TEST PROBLEMS

The proposed approach is tested first on two simulated examples. The growth term in both these examples is separable:

$$G_r(r, t) = G_1(r)G_2(t), \quad (11)$$

$$G_1(r) = \begin{cases} 1 + \frac{r}{6} & P_1, \\ \frac{r^2}{\alpha} & P_2, \end{cases} \quad (12)$$

$$G_2(t) = \begin{cases} \frac{3}{2}(1 + \exp(\frac{-t}{2})) & P_1, \\ \kappa \exp(\frac{-t}{\gamma}) & P_2, \end{cases} \quad (13)$$

where,  $G_r(r, t)$  is the growth rate with respect to the particle radius, and for the results shown here,  $\alpha = \gamma = 2$  and  $\kappa = 1$ .

The growth kernel for the first problem ( $P_1$ ) is the one used in the simulation example reported in Mahoney et al. (2002). The growth kernel in problem  $P_2$  is chosen to be nonlinear both with respect to  $G_1$  and  $G_2$ . The resulting evolution of the distribution in the first case is mainly dominated by movement towards large particle sizes with slight broadening, whereas in the second case the broadening of the distribution is more pronounced. In both problems the initial condition is a Gaussian distribution. Furthermore, it is assumed that measurements of the number density function are available at ten equally distributed time instances.

As described in Section 2.2 the initial distribution is divided into bins; here 100 bins are used. The evolution of the characteristics is extracted by applying the algorithm explained previously and perceptron neural networks are trained using this data. It was found that one hidden layer is sufficient for approximating the kernel. The number of neurons in all cases presented here is five. This is determined by an approach that is based on singular value decomposition (Sentoni et al., 1996).

The comparison between the original and the extracted growth kernels for problems  $P_1$  and  $P_2$  is depicted in Fig. 2. In both cases the extracted growth kernel compares well with the original one. The good agreement is also reflected in the comparison of the number density functions shown in Fig. 3 for  $P_1$  and in Fig. 4 for  $P_2$ .

It can be concluded from these results that separable growth rates can be reconstructed efficiently by the proposed algorithm. This was also the case with the approach of Mahoney et al. (2002). In what follows more general cases with a nonseparable growth kernel are considered.

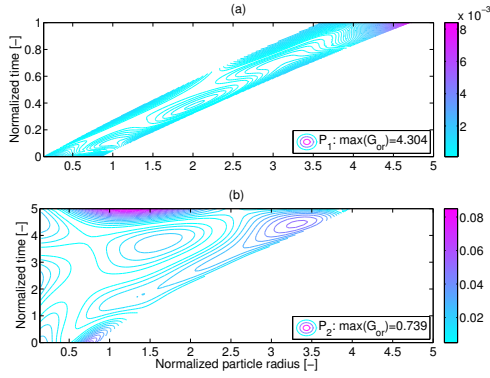


Fig. 2. Error of the extracted growth kernel in comparison with the original kernel for the test problems. The error contours are calculated from:  $E = \frac{|G_{or} - G_{ex}|}{\max(G_{or})}$ .

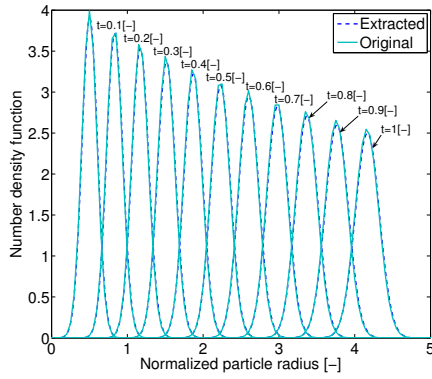


Fig. 3. Comparison of the original number density function and the number density function that results from using the extracted growth kernel for problem  $P_1$

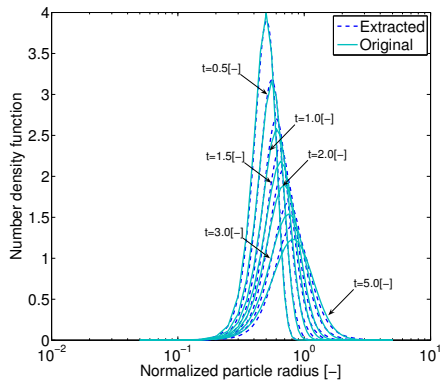


Fig. 4. Comparison of the original number density function and the number density function that results from using the extracted growth kernel for problem  $P_2$

#### 4. THE EMULSION POLYMERIZATION (EP) PROBLEM

One of the fields in which the PBE is used to describe the dynamics of a particulate system is emulsion polymerization. In this section the EP process is briefly introduced and the main aspects of the model are presented.

##### 4.1 The EP process

The main ingredients in EP are monomer, emulsifier, initiator and water. The monomer is only slightly soluble in water and it forms a separate oily phase when added to it. Upon stirring, this oily phase breaks down into monomer droplets that are unstable, and to stabilize them the emulsifier (surfactant) is added. In addition, the emulsifier is responsible for the formation of micelles which are colloidal aggregates of surfactant molecules that occur at concentrations above the critical micelle concentration. These micelles are the loci of the polymerization reaction. To ignite the reaction, a water soluble initiator is added. It forms radicals in the water phase that subsequently enter the monomer swollen micelles as oligoradicals, form polymer particles and grow by propagation. It might also occur that the monomer units add to the radicals that are generated in the aqueous phase and the propagation continues there until the solubility limit of the oligomer in water is reached. At that point, the particles precipitate and adsorb surfactant molecules to achieve their stabilization. The monomer continuously diffuses from the monomer droplets to the polymer particles during the reaction and once all the monomer present in the water, in the droplets, and in the polymer particles is consumed, the reaction terminates.

##### 4.2 The EP model

The polymer particles are of different sizes  $r$  and are located at different positions in the reactor. Assuming a well-mixed reactor, the spatial variation is neglected. The PBE that describes the evolution of the particle size distribution (PSD) then reads:

$$\frac{\partial n_r(r, t)}{\partial t} = - \frac{\partial}{\partial r} (\dot{r}(r, t) n_r(r, t)) + \mathfrak{R}_{coag}(r, t), \quad (14)$$

where  $n_r(r, t)$  is the population density function with the particle radius as the internal coordinate and  $\dot{r}(r, t)$  is the growth rate of the particles and is given by Eq. 15:

$$\dot{r}(r, t) = G_r(r, t) = \frac{k_p M W_M}{4 \pi r^2 \rho_p N_A} [M]^p \bar{n}(r, t). \quad (15)$$

In Eq. 15,  $k_p$  is the propagation rate coefficient,  $M W_M$  is the molecular weight of the monomer,  $N_A$  is Avogadro's number,  $\rho_p$  is the density of the polymer,  $[M]^p$  is the monomer concentration in the particle phase and  $\bar{n}$  is the average number of radicals per particle.

$\bar{n}(r, t)$  depends on the rate of radical generation, the concentration of the polymer particles, the rate of radical entry into the particles, the exit rate of radicals from the particles and the termination rate of the radicals. In this model, the explicit expression for  $\bar{n}(r, t)$  developed by Li and Brooks (1993) is used. Due to the nonlinear dependency of  $\bar{n}$  on both particle radius and time, the growth kernel  $G_r(r, t)$  in emulsion polymerization is nonseparable.

The PBE (Eq.14) is coupled to ordinary differential equations describing the change in the concentration of the other substances that are present in the reactor (i.e. the initiator, monomer and radicals in the water phase). This set of equations, the recipe and the experimental conditions used in this example can be found in Bouaswaig and

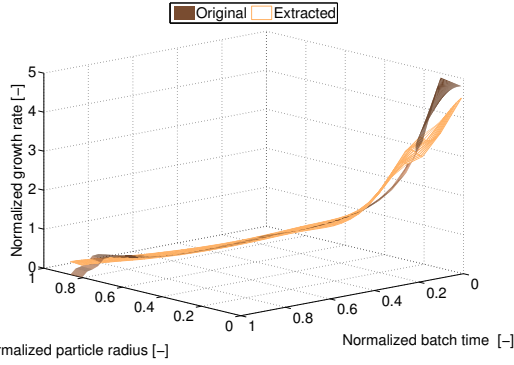


Fig. 5. Comparison of the original and the extracted growth kernels for the EP problem (growth only case).

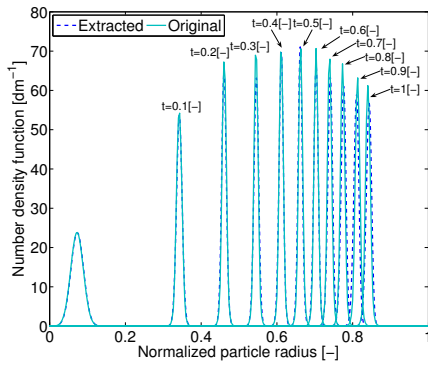


Fig. 6. Comparison of the original number density function and the number density function that results from using the extracted growth kernel for the EP problem (Growth only case).

Engell (2009).

The virtual experimental data in what follows is generated by discretizing the PBE using the improved weighted essentially non-oscillatory scheme (WENO35-Z) (Borges et al., 2008). The resulting set of equations is simulated using the DAE solver DASSL. For the inverse problems 100 bins are used; the virtual experimental data is available at ten time instances in the pure growth case and at eighty time instances in the growth and coagulation case.

#### 4.3 The EP pure growth case

For this case the coagulation term  $\mathfrak{R}_{coag}(r, t)$  in Eq. 14 is equal to zero. The calculation proceeds in the same fashion as described earlier in Section 2.2. The comparison of the extracted and the original growth kernels is shown in Fig. 5. It is clear that the growth kernel for this case is extracted with reasonable accuracy.

In Fig. 6 a comparison between the particle size density obtained from using the original and the extracted growth kernels is shown. In Fig. 7 the conversions in both cases are compared. The results in both figures reveal the suitability of the proposed algorithm for extracting this nonseparable growth kernel.

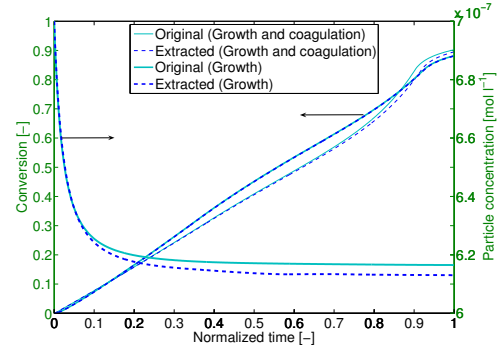


Fig. 7. Comparison of conversion and particle concentration for the pure growth EP problem and the growth and coagulation EP problem.

#### 4.4 The EP growth and coagulation case

Model mismatch in EP processes has been reported in literature (see, e.g. Immanuel et al. (2002)). Due to the complexity of the process and the strong interaction of the nucleation, growth and coagulation phenomena, validation of the complete model is impractical. Fortuny et al. (2004) proposed using pure coagulation experiments to validate the coagulation kernel separately. For a known coagulation kernel, the approach presented here can be used either to extract the growth kernel or to improve the quality of the existing rigorous model.

The coagulation coefficient  $\beta$  in this case is given by:

$$\beta(v_1, v_2) = \frac{2k_B T}{3\mu W(v_1, v_2)} \left( 2 + \frac{v_1^{1/3}}{v_2^{1/3}} + \frac{v_2^{1/3}}{v_1^{1/3}} \right), \quad (16)$$

where  $k_B$  is the Boltzmann constant,  $T$  is the reactor temperature,  $\mu$  is the viscosity of the medium and  $W(v_1, v_2)$  is the stability ratio. For  $W$  an expression similar to that used by Alexopoulos et al. (2004) is used here:

$$W(v_1, v_2) = \left( \frac{v_1 v_2}{v_{min}^2} \right)^s, \quad (17)$$

where  $v_{min}$  is the volume corresponding to the lower limit of the particle size domain and  $s$  is chosen to be equal to 1.25. Hence, it is assumed that the coagulation dynamics are known and the goal is to extract the nonseparable growth kernel.

As mentioned in Section 2.2, the set of nonlinear equations that result from applying FPMG to extract the growth kernel in this case are solved simultaneously. The accuracy of the extracted kernel is acceptable, as can be seen in Fig. 8. Furthermore, as illustrated in Fig. 7, due to the presence of coagulation, the particle concentration (i.e. amount of particles per unit volume of the reactor content) decreases over time. This is captured reasonably well by the model that uses the extracted growth kernel. The same applies to the conversion as can be concluded from the same figure. For this case however, there exists a certain discrepancy between the cumulative densities predicted by using the different kernels as can be seen in Fig. 9. When  $t$  approaches 1, the error in the location of the front is around 4% and the distribution predicted by the extracted kernel is slightly broader. This difference is attributed to the numerical error associated with the application of Steps 3.1. and 3.2. in the proposed algorithm.

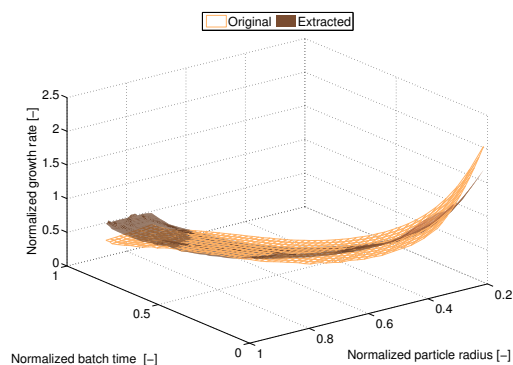


Fig. 8. Comparison of the original and the extracted growth kernels for the EP problem (growth and coagulation case).

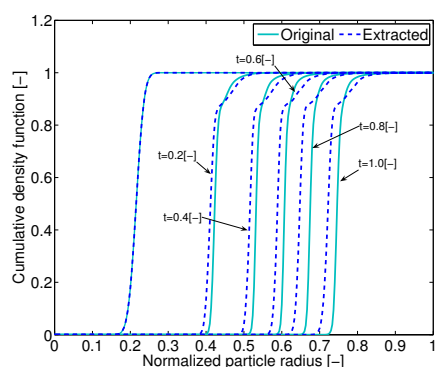


Fig. 9. Comparison of the original cumulative density function and the cumulative density function that results from using the extracted growth kernel for the EP problem (growth and coagulation case).

## 5. CONCLUSION

When measurements of the number density function at different time instances are available, the growth kernel can be extracted by constructing the characteristics that describe the evolution of the PSD. The technique presented in this paper is based on this concept and is applicable even when the assumption of separable growth kernel is not valid. When the growth is accompanied by coagulation the growth kernel can still be extracted with reasonable accuracy using the proposed algorithm, assuming the coagulation kernel to be known.

In the approach shown here the dependence of the growth kernel on the continuous phase variables is only implicitly defined via the dependence on time and this confines its value. This limitation will be addressed in future work, i.e. the growth kernel will be estimated as a function of the state variables. An additional potential direction for future research is the use of dynamic neural networks instead of a static mapping to combine Steps 4 and 5 in the algorithm presented in Section 2.2 for extracting the growth kernel.

## REFERENCES

Alexopoulos, A., Roussos, A., and Kiparissides, C. (2004). Part I: Dynamic evolution of the particle size distribution in particulate processes undergoing combined

particle growth and aggregation. *Chemical Engineering Science*, 59, 5751–5769.

Alhamad, B., Romagnoli, J., and Gomes, V. (2005). Advanced modelling and optimal operating strategy in emulsion copolymerization: Application to styrene/MMA system. *Chemical Engineering Science*, 60, 2795–2813.

Borges, R., Carmona, M., Costa, B., and Don, W. (2008). An improved weighted essentially non-oscillatory scheme for hyperbolic conservation laws. *Journal of Computational Physics*, 227, 3191–3211.

Bouaswaig, A. and Engell, S. (2009). Weno scheme with static grid adaptation for tracking steep moving fronts. *Chemical Engineering Science*, 64, 3214–3226.

Dokucu, M. and Doyle III, F. (2008). Batch-to-batch control of characteristic points on the PSD in experimental emulsion polymerization. *AIChE Journal*, 54(12), 3171–3187.

Dokucu, M., Park, M., and Doyle III, F. (2008). Reduced-order methodologies for feedback control of particle size distribution in semi-batch emulsion copolymerization. *Chemical Engineering Science*, 63, 1230–1245.

Fortuny, M., Graillat, C., and McKenna, T. (2004). Coagulation of anionically stabilized polymer particles. *Ind. Eng. Chem. Res.*, 43, 7210–7219.

Immanuel, C., Cordeiro, C., Sundaram, S., Meadows, E., Crowley, T., and Doyle III, F. (2002). Modeling of particle size distribution in emulsion co-polymerization: Comparison with experimental data and parametric sensitivity studies. *Computers and Chemical Engineering*, 26, 1133–1152.

Kumar, S. and Ramkrishna, D. (1997). On the solution of population balance equations by discretization-III. Nucleation, growth and aggregation of particles. *Chemical Engineering Science*, 52(24), 4659–4679.

Li, B. and Brooks, B. (1993). Prediction of the average number of radicals per particle for emulsion polymerization. *Journal of Polymer Science: Part A: Polymer Chemistry*, 31, 2397–2402.

Mahoney, A., Doyle III, F., and Ramkrishna, D. (2000). Inverse problem approach to modeling of particulate systems. In *Proceedings of the American control conference*, volume 3, 1727–1731.

Mahoney, A., Doyle III, F., and Ramkrishna, D. (2002). Inverse problems in population balances: Growth and nucleation from dynamic data. *AIChE Journal*, 48(5), 981–990.

Rajabi-Hamane, M. and Engell, S. (2007). Time optimal production of a specified particle size distribution in emulsion polymerization. *Chemical Engineering Science*, 62, 5282–5289.

Ramkrishna, D. (2000). *Population balances: Theory and applications to particulate systems in engineering*. Academic press, San Diego.

Sentoni, G., Agamennoni, O., Desages, A., and Romagnoli, J. (1996). Approximate models for nonlinear process control. *AIChE Journal*, 42(8), 2240–2250.

Wright, H. and Ramkrishna, D. (1992). Solutions of inverse problems in population balances-I. Aggregation kinetics. *Computers and Chemical Engineering*, 16(12), 1019–1038.